Inorg. Chem. **2006**, *45*, 8179–8187

Mono- and Polynuclear Complexes of the Model Nucleobase 1-Methylcytosine. Synthesis and Characterization of *cis*-$[(PMe_2Ph)_2Pt\{(1\text{-}MeCy(-H)\}]_3(NO_3)_3$ and *cis*-$[(PPh_3)_2Pt\{1\text{-}MeCy(-H)\}(1\text{-}MeCy)]NO_3$

Bruno Longato,*,†,‡ Diego Montagner,‡ and Ennio Zangrando§

Istituto di Scienze e Tecnologie Molecolari, CNR, c/o Dipartimento di Scienze Chimiche, Università di Padova, Via Marzolo 1, 35131 Padova, Italy, Dipartimento di Scienze Chimiche, Università di Padova, Via Marzolo 1, 35131 Padova, Italy, and Dipartimento di Scienze Chimiche, Università di Trieste, Via Giorgieri 1, 34127 Trieste, Italy

Received May 15, 2006

The hydroxo complex *cis*-$[L_2Pt(\mu\text{-}OH)]_2(NO_3)_2$ (L = PMe_2Ph), in various solvents, reacts with 1-methylcytosine (1-MeCy) to give as the final product the cyclic species *cis*-$[L_2Pt\{1\text{-}MeCy(-H),N^3N^4\}]_3(NO_3)_3$ (**1**) in high or quantitative yield. X-ray analysis of **1** evidences a trinuclear species with the NH_2-deprotonated nucleobases bridging *symmetrically* the metal centers through the N3 and N4 donors. A multinuclear NMR study of the reaction in DMSO-d_6 reveals the initial formation of the dinuclear species *cis*-$[L_2Pt\{1\text{-}MeCy(-H),N^3N^4\}]_2^{2+}$ (**2**), which quantitatively converts into **1** following a first-order kinetic law (at 50 °C, $t_{1/2}$ = 5 h). In chlorinated solvents, the deprotonation of the nucleobase affords as the major product (60–70%) the linkage isomer of **1**, *cis*-$[L_2Pt\{1\text{-}MeCy(-H)\}]_3^{3+}$ (**3**), in which three cytosinate ligands bridge *unsymmetrically* three *cis*-L_2Pt^{2+} units. In solution, **3** slowly converts quantitatively into the thermodynamically more stable isomer **1**. No polynuclear adducts were obtained with the hydroxo complex stabilized by PPh_3. *cis*-$[(PPh_3)_2Pt(\mu\text{-}OH)]_2(NO_3)_2$ reacts with 1-MeCy, in DMSO or CH_2Cl_2, to give the mononuclear species *cis*-$[(PPh_3)_2Pt\{1\text{-}MeCy(-H)\}(1\text{-}MeCy)](NO_3)$ (**4**) containing one neutral and one NH_2-deprotonated 1-MeCy molecule, coordinated to the same metal center at the N3 and N4 sites, respectively. X-ray analysis and NMR studies show an intramolecular H bond between the N4 amino group and the uncoordinated N3 atom of the two nucleobases.

Introduction

Cytosine, as a neutral molecule, can exist in six tautomeric forms. Structural, spectroscopic, and theoretical studies indicate that tautomer **I** (Chart 1, R = H) is largely the most dominant.[1] Alkylation at N1 reduces the number of possible tautomers to three (**I**−**III** in Chart 1). The basicity of N3 (pK_a = 4.6) favors this cytosine atom as the primary site for metal coordination.[2] However, examples of the rare imino−oxo tautomer (**II** in Chart 1) of 1-methylcytosine, through N4 coordination to Pt^{IV} [3] and Pt^{II},[4] are also known.

Chart 1

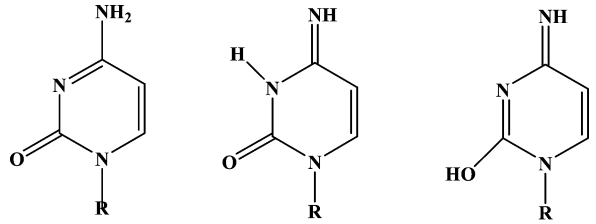

I **II** **III**

* To whom correspondence should be addressed. E-mail: bruno.longato@unipd.it.
† Istituto di Scienze e Tecnologie Molecolari, CNR.
‡ Università di Padova.
§ Università di Trieste.

(1) Taylor, R.; Kennard, O. *J. Mol. Struct.* **1982**, *78*, 1. Bandekar, J.; Zundel, G. *Spectrochim. Acta, Part A* **1983**, *39*, 343. Scanlan, M. J.; Hillier, I. M. *J. Am. Chem. Soc.* **1984**, *106*, 3737.
(2) Lippert, B. *Prog. Inorg. Chem.* **1989**, *37*, 1.
(3) Lippert, B.; Schöllhorn, H.; Thewalt, U. *J. Am. Chem. Soc.* **1986**, *108*, 6616.
(4) Pichierri, F.; Holthenrich, D.; Zangrando, E.; Lippert, B.; Randaccio, L. *J. Biol. Inorg. Chem.* **1996**, *1*, 439.

10.1021/ic060831r CCC: $33.50
Published on Web 09/09/2006

Chart 2

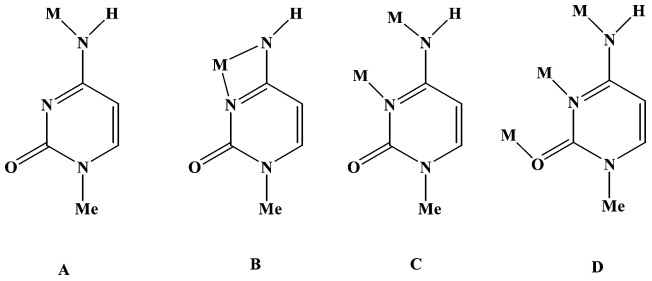

Chart 3

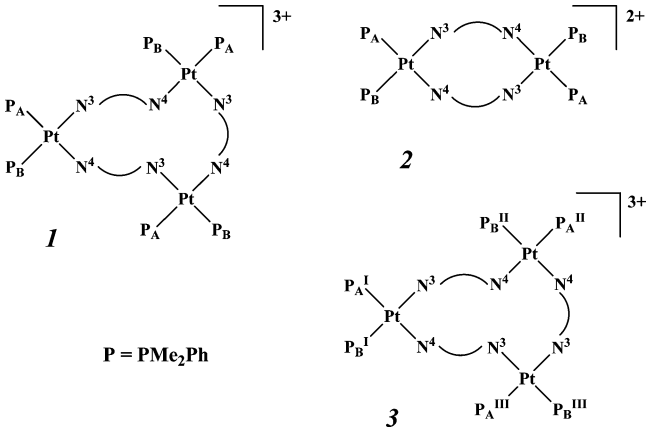

Deprotonation of the exocyclic NH_2 group ($pK_a = 16.7$)[5] leads the anion to behave as mono-, bi-, and tridentate ligands, as shown in Chart 2, which summarizes the binding modes of the 1-methylcytosinate ion [1-MeCy(−H)]. The anion has been found to act as a monodentate ligand through N4 (**A** mode), binding metal centers in high oxidation states such as Pt^{IV} [6] and Ru^{III} [7] or, more frequently, as a bidentate ligand, coordinating the same metal ion in a chelating fashion (**B** mode) or bridging two metal centers through N3 and N4 donors (**C** mode).[8] Cytosinate anions have been shown to act also as tridentate ligands (**D** mode) in trinuclear $PtPd_2$ and $PtAg_2$ complexes.[9]

We have found that if deprotonation of 1-MeCy is performed through the hydroxo complex *cis*-$[(PMe_3)_2Pt(\mu\text{-}OH)]_2^{2+}$, the cytosinate ion binds two metal centers exclusively through the N3 and N4 atoms (**C** mode) to form the dinuclear species *cis*-$[(PMe_3)_2Pt\{1\text{-}MeCy(-H),N^3N^4\}]_2^{2+}$, with the nucleobases bridging the metal centers in a *head-to-tail* fashion.[10] This complex, in dimethyl sulfoxide (DMSO) or H_2O at 80 °C, converts into the corresponding trinuclear derivative *cis*-$[(PMe_3)_2Pt\{1\text{-}MeCy(-H),N^3N^4\}]_3^{3+}$, in which the anionic ligands maintain the same *head-to-tail* arrangement.[11] Cyclic trimers of Pt^{II} stabilized by phosphines are rare,[12] and this derivative of 1-MeCy appears to be the only one structurally characterized.[13] Very recently, a Pd analogue, stabilized by *N*,*N*,*N*′,*N*′-tetramethylethylenediamine, has been described by Lippert et al.[14]

In this paper, we report a detailed analysis of the interactions of the hydroxo complexes *cis*-$[L_2Pt(\mu\text{-}OH)]_2^{2+}$ (L = PMe_2Ph and PPh_3), with 1-MeCy showing that the cytosinate anion forms trinuclear adducts when L is PMe_2Ph. The thermodynamically stable product is the cyclic species *cis*-$[(PMe_2Ph)_2Pt\{1\text{-}MeCy(-H),N^3N^4\}]_3^{3+}$ (**1**; Chart 3), characterized by a single-crystal X-ray analysis structurally similar to that of the PMe_3 complex.[11] When the condensation reaction is monitored in DMSO, the cyclic intermediate *cis*-$[(PMe_2Ph)_2Pt\{1\text{-}MeCy(-H),N^3N^4\}]_2^{2+}$ (**2**) has been identified and its conversion to **1** investigated. However, when the condensation reaction is performed in chlorinated solvents, the main product is the linkage isomer of **1**, i.e., the cyclic species *cis*-$[(PMe_2Ph)_2Pt\{1\text{-}MeCy(-H)\}]_3^{3+}$ (**3**; Chart 3), where the bridging nucleobases bind the metal centers *unsymmetrically*. A complete characterization of this unprecedented trinuclear species has been obtained by multinuclear NMR analysis and its stability in solution investigated. Moreover, the extension of this study to the hydroxo complex stabilized by PPh_3 shows that similar polynuclear complexes of 1-MeCy are unstable. Instead, the mononuclear bis-adduct *cis*-$[(PPh_3)_2Pt\{1\text{-}MeCy(-H)\}(1\text{-}MeCy)]^+$ (**4**) is formed in high yield. This compound, structurally characterized by single-crystal X-ray analysis, represents the first example of a 1-MeCy complex where one neutral and one NH_2-deprotonated nucleobase are coordinated to the same metal center.

Experimental Section

Instrumentation and Materials. ^1H, $^{13}C\{^1H\}$, and $^{31}P\{^1H\}$ NMR spectra were recorded at 27 °C on a Bruker AVANCE 300 and/or Bruker 600 MHz, while 2D $^{15}N-^1H$ and $^{31}P-^1H$ NMR spectra were recorded at 27 °C on a Bruker 400 AMX-WB spectrometer (at 40.56, 75.47, and 161.49 MHz, respectively) and were calibrated against the residual signals of the solvent (for ^1H and ^{13}C NMR) and external H_3PO_4 for ^{31}P NMR. The external references for ^{195}Pt and ^{15}N were Na_2PtCl_4 in D_2O (adjusted to δ −1628 ppm from Na_2PtCl_6) and CH_3NO_2, respectively. Inverse-detected spectra were obtained through heteronuclear multiple-quantum or multiple-bond correlation (HMQC or HMBC) experiments, using parameters similar to those previously reported.[15] Deuterated solvents (from Aldrich) were used as received. 1-MeCy,[16]

(5) Lippert, B. *Handbook of Nucleobase Complexes*; Lusty, J. R., Ed.; CRC Press: Boca Raton, FL, 1990; Vol. 1, p 9.
(6) Randaccio, L.; Zangrando, E.; Cesàro, A.; Holthenrich, D.; Lippert, B. *J. Mol. Struct.* **1998**, *440*, 221.
(7) Graves, B. J.; Hodgson, D. J. *J. Am. Chem. Soc.* **1979**, *101*, 5608.
(8) Zangrando, E.; Pichierri, F.; Randaccio, L.; Lippert, B. *Coord. Chem. Rev.* **1996**, *156*, 275.
(9) (a) Holthenrich, D.; Krumm, M.; Zangrando, E.; Pichierri, F.; Randaccio, L.; Lippert, B. *J. Chem. Soc., Dalton Trans.* **1995**, 3275. (b) Holthenrich, D.; Zangrando, E.; Chiarparin, E.; Lippert, B.; Randaccio, L. *J. Chem. Soc., Dalton Trans.* **1997**, 4407.
(10) Trovò, G.; Bandoli, G.; Casellato, U.; Corain, B.; Nicolini, M.; Longato, B. *Inorg. Chem.* **1990**, *29*, 4616.
(11) Schenetti, L.; Bandoli, G.; Dolmella, A.; Trovò, G.; Longato, B. *Inorg. Chem.* **1994**, *33*, 3169.
(12) (a) Schweiger, M.; Seidel, S. R.; Arif, A. M.; Stang, P. J. *Angew. Chem., Int. Ed.* **2001**, *40*, 3467. (b) Schweiger, M.; Seidel, S. R.; Arif, A. M.; Stang, P. J. *Inorg. Chem.* **2002**, *41*, 2556. (c) Longato, B.; Pasquato, L.; Mucci, A.; Schenetti, L.; Zangrando, E. *Inorg. Chem.* **2003**, *42*, 7861.
(13) Randaccio, L.; Zangrando, E. In *Cisplatin—Chemistry and Biochemistry of a Leading Anticancer Drug*; Lippert, B., Ed.; VHCA: Zürich, Switzerland, 1999; pp 405−428.
(14) Shen, W.-Z.; Gupta, D.; Lippert, B. *Inorg. Chem.* **2005**, *44*, 8249.
(15) Schenetti, L.; Mucci, A.; Longato, B. *J. Chem. Soc., Dalton Trans.* **1996**, 299.
(16) Kistenmacher, T. J.; Rossi, M.; Caradonna, J. P.; Marzilli, L. G. *Adv. Mol. Relax. Interact. Processes* **1979**, *15*, 119.

cis-$[(PMe_2Ph)_2Pt(\mu\text{-}OH)]_2(NO_3)_2$,[17] and *cis*-$[(PPh_3)_2Pt(\mu\text{-}OH)]_2(NO_3)_2$[18] were synthesized as previously reported.

Synthetic Work. 1. *cis*-$[(PMe_2Ph)_2Pt\{1\text{-}MeCy(-H),N^3N^4\}]_3(NO_3)_3$ (1). A suspension of *cis*-$[(PMe_2Ph)_2Pt(\mu\text{-}OH)]_2(NO_3)_2$ (201 mg, 0.183 mmol) and 1-MeCy (45.9 mg, 0.366 mmol) in H_2O (5 mL) was stirred at room temperature for ca. 1 h. The resulting colorless solution, stored overnight at 10 °C, separated a white amorphous solid, which was recovered by filtration and dissolved in a mixture of H_2O (0.5 mL) and EtOH (1 mL). Slow evaporation of the solution afforded a crystalline solid, which was recovered by filtration and dried under vacuum. The elemental analysis and ^{1}H NMR indicate the presence of a molecule of water for each Pt atom. The yield of **1**·3H_2O was 197 mg (55%). Elem anal. Calcd for $C_{21}H_{28}N_4O_4P_2Pt\cdot H_2O$: C, 37.34; H, 4.48; N, 8.30. Found: C, 37.70; H, 4.42; N, 8.23. A better yield of **1** was obtained when the reaction was carried out in acetonitrile as follows. A suspension of *cis*-$[(PMe_2Ph)_2Pt(\mu\text{-}OH)]_2(NO_3)_2$ (236 mg, 0.214 mmol) and 1-MeCy (53.6 mg, 0.428 mmol) in CH_3CN (6 mL) was stirred at room temperature. In a few minutes, a colorless solution was obtained and was left to stand overnight at room temperature and then filtered to eliminate trace amounts of Pt. The addition of Et_2O afforded a white solid, which was filtered, washed with Et_2O, and dried under vacuum. Dissolution of the crude product in CH_3CN followed by slow condensation of Et_2O vapors afforded a crystalline solid (216 mg, yield 81%) having the composition **1**·H_2O·CH_3CN. ^{1}H and ^{31}P NMR data are collected in Tables 3 and 4, respectively. $\{^1H\}^{13}C$ NMR (in $CDCl_3$ at 27 °C): 165.94 (d, $^3J_{CP}$ = 4.5 Hz, C-4), 156.60 (d, $^3J_{CP}$ = 2 Hz, C-2), 143.97 (s, C-6), 133.18−130.17 (complex set of overlapping doublets, PMe_2*Ph*), 99.35 (s, C-5), 38.90 (s, N*C*H_3); 15.39 (d, $^1J_{CP}$ = 42.6 Hz, P*Me*$_2$Ph), 14.44 (d, $^1J_{CP}$ = 43.3 Hz, P*Me*$_2$Ph), 13.81 (d, $^1J_{CP}$ = 41.2 Hz, P*Me*$_2$Ph), 15.51 (dd, $^1J_{CP}$ = 42.5 Hz, $^3J_{CP}$ = 1.7 Hz, P*Me*$_2$Ph). The inverse-detected ^{195}Pt NMR resonance in $CDCl_3$ showed the expected doublet of doublets pattern at δ −4314 ppm, with $^1J_{PtP}$ values consistent with those measured in the corresponding ^{31}P NMR spectrum. ^{15}N (inverse-detected) NMR data in $CDCl_3$ (δ, ppm): −245 N(1); −258 ($^1J_{NH}$ = 75 Hz, $^2J_{NP}$ = 70 Hz) N(4). [The electrospray ionization (ESI) spectrum is depicted in the Supporting Information, Figure S1].

2. *cis*-$[(PMe_2Ph)_2Pt\{1\text{-}MeCy(-H)\}]_3^{3+}$ (3). A mixture of *cis*-$[(PMe_2Ph)_2Pt(\mu\text{-}OH)]_2(NO_3)_2$ (132 mg, 0.12 mmol) and 1-MeCy (30 mg, 0.24 mmol) in CH_2Cl_2 (3 mL) was stirred at room temperature for ca. 1 h at 0 °C. A small amount of the solid phase was eliminated by filtration, and the addition of Et_2O (30 mL) afforded a white precipitate, which was collected by filtration and dissolved again in CH_2Cl_2. Fractional precipitation with Et_2O afforded two portions of precipitate, which were analyzed by ^{31}P NMR, in fresh prepared $CDCl_3$ solutions. The composition of the first fraction (ca. 80 mg), expressed as a contribution of the integrals of each species (see Table 4), was as follows: complex **3** (58%), complex **1** (32%), unreacted hydroxo complex (2%), and unattributed resonances (8%). The composition of the second fraction (ca. 50 mg) was as follows: **3** (72%), **1** (14%), unreacted hydroxo (12%), and unattributed resonaces (2%). This latter sample was used for the ^{195}Pt (inverse-detected) NMR experiment. (δ, ^{195}Pt): for Pt^I, −4320 ppm; for Pt^{II}, −4261 ppm.

3. *cis*-$[(PPh_3)_2Pt\{1\text{-}MeCy(-H)\}(1\text{-}MeCy)]NO_3$ (4). 1-MeCy (64 mg, 0.51 mmol) was added to a solution of *cis*-$[(PPh_3)_2Pt(\mu\text{-}OH)]_2(NO_3)_2$ (204 mg, 0.125 mmol) in a mixture of CH_2Cl_2 (4 mL) and $CHCl_3$ (4 mL), and the suspension was stirred at room temperature for ca. 15 h. The resulting solid was recovered by filtration, washed twice with $CHCl_3/CH_2Cl_2$ (1:1), and purified by dissolution in *N*,*N*-dimethylformamide (DMF) and precipitation with Et_2O. The yield of the dried solid, having the composition **4**·H_2O·DMF, was 158 mg (56%). Elem anal. Calcd for $C_{46}H_{43}N_7O_5P_2Pt\cdot H_2O\cdot$DMF: C, 52.45; H, 4.67; N, 9.98. Found: C, 52.73; H, 4.53; N, 10.01. ^{1}H NMR in DMSO-d_6 (δ, ppm): 7.89−7.85 (c.m., 4H, P*Ph*), 7.64−7.16 (c.m., 11H, P*Ph* and H6 of 1-MeCy(−H)). 1-MeCy(−H) resonances: 5.07 (d, $^3J_{HP}$ = 4.7 Hz, 1H, N*H*), 4.98 (d, $^3J_{HH}$ = 7.3 Hz, 1H, H5), 3.11 (s, 3H, NCH_3). 1-MeCy resonances: 10.63 (s, 1H, N*H*), 8.34 (s, 1H, N*H*), 6.66 (d, $^3J_{HH}$ = 7.3 Hz, 1H, H6), 5.25 (dd, $^3J_{HH}$ = 7.3 Hz, $^5J_{HP}$ = 1.6 Hz, 1H, H5), 3.18 (s, 3H, NCH_3). $\{^1H\}^{31}$P NMR in DMSO-d_6: AB multiplet at δ 12.34 ($^1J_{PPt}$ = 3241 Hz) and 0.21 ($^1J_{PPt}$ = 3452 Hz) with $^2J_{PP}$ = 20.1 Hz. ^{195}Pt (inverse-detected) NMR data in DMSO-d_6 (δ, ppm): −4825 ppm.

^{1}H NMR in DMF-d_7 (δ, ppm): 7.789−7.24 (c.m., 31H, P*Ph* and H6 of 1-MeCy(−H)). 1-MeCy(−H) resonances: 5.15 (d, $^3J_{HH}$ = 6.8 Hz, 1H, H5), 5.11 (d, $^3J_{HP}$ = 4.4 Hz, 1H, N*H*), 3.27 (s, 3H, NCH_3). 1-MeCy resonances: 10.94 (s, 1H, N*H*), 8.39 (s, 1H, N*H*), 6.77 (d, $^3J_{HH}$ = 7.2 Hz, 1H, H6), 5.49 (dd, $^3J_{HH}$ = 7.2 Hz, $^5J_{HP}$ = 1.7 Hz, 1H, H5), 3.19 (s, 3H, NCH_3). $\{^1H\}^{31}$P NMR in DMF- d_7: AB multiplet at δ 12.74 ($^1J_{PPt}$ = 3192 Hz) and 0.90 ($^1J_{PPt}$ = 3597 Hz) with $^2J_{PP}$ = 20.2 Hz.

4. Kinetic Study of the Conversion of *cis*-$[(PMe_2Ph)_2Pt\{1\text{-}MeCy(-H),N^3N^4\}]_2(NO_3)_2$ (2) into 1. A 5-mm NMR tube was loaded with a solution of *cis*-$[(PMe_2Ph)_2Pt(\mu\text{-}OH)]_2(NO_3)_2$ (14.2 mg) and 1-MeCy (3.2 mg) in DMSO-d_6 (1 mL). The ^{31}P NMR spectrum, obtained at 27 °C, was similar to that reported in Figure 3a, where the content of **2** was ca. 90%. The temperature of the sample was then brought to 50 °C, and the ^{31}P NMR spectra (1500 scans) were obtained at intervals of 2−5 h. The relative molar concentrations of **1** and **2** were measured from the integrals of the pertinent species. A linear dependence of ln([**1**]/[**2**]) vs time was obtained (see the Supporting Information, Figure S2), and the calculated value of $t_{1/2}$ was ca. 5 h.

X-ray Structure Determinations. Diffraction data for compound **1** were collected on a Nonius DIP-1030H system equipped with Mo Kα radiation [λ = 0.710 73 Å; T = 293(2) K] and those of **4** at the RX diffraction beamline [λ = 1.000 00 Å; T = 100(2) K] of Elettra synchrotron (Trieste, Italy). Cell refinement, indexing, and scaling of the data sets were carried out using Denzo and Scalepack.[19] Both of the structures were solved by direct method and subsequent Fourier analyses and refined by the full-matrix least-squares methods based on F^2 with all observed reflections.[20] The ΔF maps evidenced some residuals interpreted as a water O and an acetonitrile molecule in **1**, while the crystal of **4** contained a water and a DMF molecule per complex unit. The program VOID (Platon package) evidenced in **1** a residual potential solvent volume that accounts for the 14.2% of the unit cell. H atoms were located at geometrical positions; those of cytosine exocyclic amino groups and of water of **4** were derived from the Fourier map. H atoms of the disordered solvent species of **1** were not included. All of the calculations were performed using the WinGX System, version 1.70.05.[21] Crystallographic data are collected in Table 1.

(17) Longato, B.; Pasquato, L.; Mucci, A.; Schenetti, L. *Eur. J. Inorg. Chem.* **2003**, 128.
(18) Longato, B.; Montagner, D.; Bandoli, G.; Zangrando, E. *Inorg. Chem.* **2006**, *45*, 1805.
(19) Otwinowski, Z.; Minor, W. Processing of X-ray Diffraction Data Collected in Oscillation Mode. *Methods in Enzymology, Volume 276: Macromolecular Crystallography*; Carter, C. W., Jr., Sweet, R. M., Eds.; Academic Press: New York, 1997; Part A, pp 307−326.
(20) *SHELX97, Programs for Crystal Structure Analysis*, release 97-2; University of Göttingen: Göttingen, Germany, 1998.
(21) Farrugia, L. J. *J. Appl. Crystallogr.* **1999**, *32*, 837.

Table 1. Crystallographic Data and Details of Structure Refinements for Compounds **1** and **4**

	1·H_2O·CH_3CN	**4**·H_2O·DMF
formula	$C_{65}H_{89}N_{13}O_{13}P_6Pt_3$	$C_{49}H_{52}N_8O_7P_2Pt$
M_r	2031.58	1122.02
cryst syst	triclinic	monoclinic
space group	$P\bar{1}$	$P2_1/c$
a (Å)	14.969(4)	13.190(3)
b (Å)	15.766(4)	38.648(5)
c (Å)	21.517(5)	9.754(3)
α (deg)	74.31(3)	
β (deg)	74.71(2)	110.30(2)
γ (deg)	62.19(2)	
V (Å^3)	4267.4(19)	4663.5(19)
Z	2	4
D_{calcd} (g cm^{-3})	1.581	1.598
Mo Kα (mm^{-1})	5.078	4.712
F(000)	1996	2264
θ_{max} (deg)	28.41	31.72
reflns collected	26 464	22 826
unique reflns	17 974	5073
R_{int}	0.0589	0.0313
obsd $I > 2\sigma(I)$	9314	4744
no. of param	887	619
GOF (F^2)	0.870	1.070
R1 [$I > 2\sigma(I)$][a]	0.0566	0.0288
wR2[a]	0.1256	0.0773
residuals (e Å^{-3})	1.666, −2.387	0.562, −0.894

[a] $R1 = \sum||F_o| - |F_c||/\sum|F_o|$; $wR2 = [\sum w(F_o^2 - F_c^2)^2/\sum w(F_o^2)^2]^{1/2}$.

Results and Discussion

Synthesis and Characterization of *cis*-[L_2Pt{1-MeCy(−H),N^3N^4}]$_3$(NO_3)$_3$ (L = PMe_2Ph, 1). The hydroxo complex *cis*-[L_2Pt(μ-OH)]$_2$(NO_3)$_2$ (L = PMe_2Ph) reacts with 1-MeCy, in a variety of solvents, to give the trinuclear species *cis*-[L_2Pt{1-MeCy(−H),N^3N^4}]$_3$(NO_3)$_3$ (**1**), according to reaction 1. In CH_3CN at room temperature, the reaction is

$$3(cis\text{-}[L_2Pt(\mu\text{-}OH)]_2^{2+}) + 6(1\text{-}MeCy) \rightarrow 2(cis\text{-}[L_2Pt\{1\text{-}MeCy(\text{-}H),N^3N^4\}]_3^{3+}) + 6H_2O \quad (1)$$

complete in 2−3 h, with 95% yield of **1** (by NMR). In H_2O, DMSO, or chlorinated solvents, a longer reaction time is required (several hours or days), and the yield is virtually quantitative.

Crystals separated from CH_3CN have the composition **1**·H_2O·CH_3CN. The X-ray structure analysis evidences the formation of a trinuclear cyclic species of pseudo 3-fold symmetry, having (PMe_2Ph)$_2$Pt units symmetrically bridged by the cytosinate ligands through the N3 and N4 atoms, thus forming a 12-membered ring as shown in Figure 1. The formation of the cyclic cation is attained, for each nucleobase, through an anti orientation of the metal at N4 with respect to that bound to N3.

Each Pt atom completes the distorted square-planar coordination geometry through two phosphine ligands. The Pt−N3 bond distances [2.093(8), 2.108(7), and 2.138(7) Å] appear to be slightly longer with respect to the Pt−N4 ones [2.084(7), 2.075(8), and 2.100(7) Å], while the Pt−P bond distances fall in the usual range for Pt complexes and vary from 2.254(3) to 2.281(3) Å (Table 2). The metals outline a triangle with slightly different edges, with the intermetallic Pt1···Pt3 and Pt2···Pt3 distances being comparable within their estimated standard deviations [5.308(1) and 5.287(1) Å, respectively], while Pt1···Pt2 appears to be slightly shorter, at 5.174(2) Å. The whole complex presents structural features very similar to those of the *cis*-[(PMe_3)$_2$Pt{1-MeCy(−H),N^3N^4}]$_3^{3+}$ analogue[11] and of [(tmeda)Pd{1-MeCy(−H),N^3N^4}]$_3^{3+}$ (tmeda = *N*,*N*,*N*′,*N*′-tetramethylethylenediamine),[14] where the mean intermetallic distances are 5.325 and 5.170 Å, respectively.

The pyrimidine rings lie on the same side of the plane defined by the metals, making dihedral angles with the Pt_3 plane of 79.2(1)° (ring a), 66.3(2)° (ring b), and 54.9(1)° (ring c). Conversely, the N_2P_2 mean coordination planes of Pt1, Pt2, and Pt3 are inclined by 51.5(1), 46.5(1), and 38.2(1)°, respectively, with respect to the metal plane, and the cation can be regarded as a double-pinched cone (Figure 2). The crystal packing evidences a nitrate anion inside the area delimited by the coordination metal planes on the side of the P atoms, with an O pointing toward the center of the complex, interacting with the exocyclic N4 nucleobase atoms. The N4−ONO_2 distances are 3.17, 2.96, and 2.99 Å, with H atoms (at calculated geometrical positions) of N4 pointing toward this O. Thus, these complexes act as anion receptors, and a similar interaction has been detected for the perchlorate anion in the crystal structures of *cis*-[(PMe_3)$_2$Pt{1-MeCy(−H)},N^3N^4]$_3^{3+}$ and of [(tmeda)Pd{1-MeCy(−H),N^3N^4}]$_3^{3+}$, where the measured N4−$OClO_3$ mean distances are 3.14 and 3.08 Å, respectively. This feature was also observed in the two crystallographically independent cations of *cis*-[($PMePh_2$)$_2$Pt{9-MeAd(−H),N^1N^6}]$_3^{3+}$, where a nitrate was found to approach each trinuclear complex.[12c]

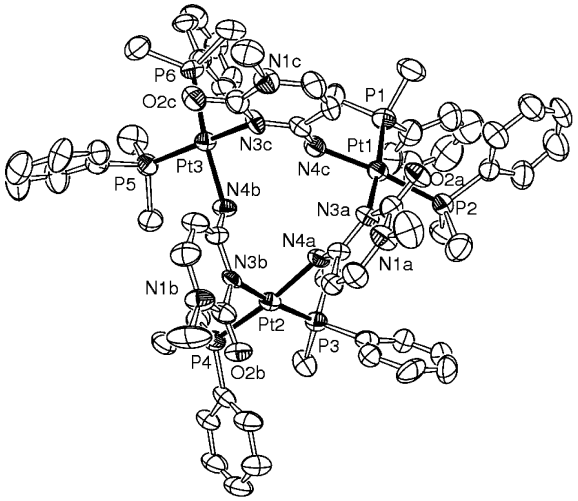

Figure 1. ORTEP drawing (ellipsoid at the 40% probability level) of the cation of **1**. C atoms are not labeled for the sake of clarity.

Table 2. Selected Coordination Bond Distances (Å) and Angles (deg) for **1**

Pt1−P1	2.254(3)	Pt2−N3b	2.108(7)
Pt1−P2	2.281(3)	Pt2−N4a	2.075(8)
Pt1−N3a	2.093(8)	Pt3−P5	2.265(3)
Pt1−N4c	2.084(7)	Pt3−P6	2.266(3)
Pt2−P3	2.267(2)	Pt3−N3c	2.138(7)
Pt2−P4	2.259(3)	Pt3−N4b	2.100(7)
N3a−Pt1−P1	173.1(2)	N3b−Pt2−P3	172.6(2)
N4c−Pt1−P2	174.3(3)	N3c−Pt3−P5	169.3(2)
N4a−Pt2−P4	173.2(2)	N4b−Pt3−P6	172.8(2)

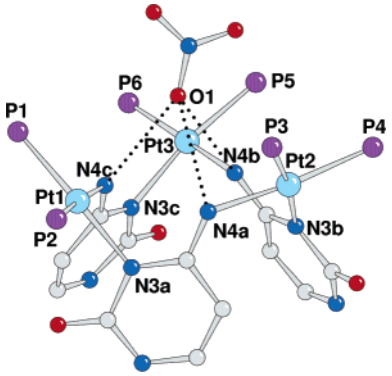

Figure 2. View of the nitrate anion interacting with N4−H atoms of the cation **1** (methyl and phenyl groups at P are not shown for clarity).

The trinuclear structure of **1** is maintained in solution, as indicated by mass spectrometry and multinuclear NMR analyses (^{1}H, ^{13}C, ^{31}P, and ^{15}N). The ESI spectrum in CH_3CN (shown in Figure S1 of the Supporting Information) exhibits a pattern with the corrected isotopic distribution, at *m*/*z* value of 1909, attributable to the monocation $\{[(PMe_2Ph)_2Pt\{1\text{-MeCy}(-H)\}]_3(NO_3)_2\}^+$. ^{1}H and ^{31}P{^{1}H} NMR data in various solvents, collected in Tables 3 and 4, respectively, show the presence of a single species, indicating a high stability of the trinuclear cation. In the ^{31}P NMR spectra, the two chemically inequivalent phosphines display an AB pattern with distinct $^1J_{PPt}$ values, which change only to a minor extent with the solvent.

In the proton spectra (Table 3), the cytosine ligands exhibit a doublet of doublets pattern for H5, resulting in a coupling with H6 ($^3J_{HH}$ = 7.5 Hz) and with one of the ^{31}P nuclei ($^5J_{HP}$ = 1.0−1.6 Hz). 2D ^{31}P−^{1}H NMR experiments in $CDCl_3$ indicate that H5 correlates with the resonance at δ −21.11 ppm, attributable to the phosphine (P_B) in the trans position to the cytosine N3 atom. This attribution stems on the assumption that the magnetic interaction ^{1}H−^{31}P through five bonds is favored via the N3 atom rather than the N4 atom. Consequently, the exocyclic N having a shorter distance (Pt−N4 = 2.086 Å, average) is trans to the phosphine that experiences the lower coupling with the metal (P_A, δ −17.83 ppm, $^1J_{PPt}$ = 3221 Hz).

As expected on the basis of the X-ray structure, the two methyl groups on the same phosphine exhibit distinct ^{1}H and ^{13}C NMR resonances (see the Experimental Section) because the coordination planes of the Pt atoms lack any symmetry. The 2D ^{31}P−^{1}H NMR spectrum, obtained in $CDCl_3$, allows the assignment of each P*Me* signal to a specific P atom, showing that the methyl groups on the same P experience chemical shift differences up to 0.43 ppm. Moreover, the magnetic anisotropy due to the presence of phenyl rings causes a marked deshielding of a methyl group in a phosphine and an opposite effect in the other one.

From Table 3, it is clear that some resonances of the nucleobases exhibit a remarkable solvent effect, in particular for the N4−H proton, observed at δ 6.82 ppm in $CDCl_3$ and at δ 5.50 ppm in CD_3CN. This is likely related to H bond interactions between the N4−H protons and the counterions, as shown in the solid state of **1** and as recently reported for the structurally similar Pd^{II} complex.[14] We observe, in fact, that the addition of chloride (as $[AsPh_4]Cl$) to solutions of **1** determines an immediate shift, in opposite directions, of the ^{31}P NMR resonances concomitant with the disappearance of the N4−H signal (shifted on the phenyl region of PMe_2Ph and $[AsPh_4]^+$) and only minor shifts (ca. 0.02 ppm) for H5 and H6 and for methyl resonances of the phosphino ligands. As an example, a solution of ca. 10^{-2} M of **1** in DMSO-d_6 containing Cl^- (molar ratio Cl^-/**1** = 2), the observed chemical shift differences were −0.34 and +0.83 ppm for the ^{31}P NMR resonances at δ −16.54 and −19.44 ppm, respectively. The fact that the values of $^1J_{PPt}$ change only a few hertz upon the addition of Cl^- seems to exclude the coordination of the chloride at the metal center.

Characterization of the *Head-to-Tail* Dimer 2. Previous studies showed that the reaction of *cis*-$[(PMe_3)_2Pt(\mu\text{-OH})]_2(NO_3)_2$ with 1-MeCy, in water or DMSO, affords the dinuclear complex *cis*-$[(PMe_3)_2Pt\{1\text{-MeCy}(-H)N^3,N^4\}]_2(NO_3)_2$, in which the cytosinate ligands bridge the metal centers through the N3 and N4 atoms in a *head-to-tail* fashion.[10] This species, in H_2O or DMSO, at 80 °C in several hours, converts into the corresponding trinuclear derivative, structurally analogous to **1**.[11] A similar dimer, **2**, is an intermediate in the formation of **1**. The ^{31}P NMR spectrum of a freshly prepared solution of *cis*-$[(PMe_2Ph)_2Pt(\mu\text{-OH})]_2(NO_3)_2$ and 1-MeCy in DMSO-d_6 is shown in Figure 3a. The AB multiplet of **2**, whose data are collected in Table 4, with a relative intensity of ca. 90%, is quantitatively replaced by the resonances of **1** in several days at ambient temperature (Figure 3b,c). A kinetic study of this transformation, carried out at ca. 50 °C, indicates a first-order kinetic law, with $t_{1/2}$ ca. 5 h. In addition, parts a and b of Figure 3 show the presence of weak resonances [at δ −16.8 (d) and −17.8 ppm (d, $^2J_{PP}$ = 22.2 Hz) and δ −18.1 (d) and −20.3 ppm (d, $^2J_{PP}$ = 24.3 Hz) and apparent singlets at δ −23.7 and −24.16 ppm], whose relative intensities undergo only small changes during the conversion of **2** into **1**. Because these signals disappear when the conversion of **2** is complete (Figure 3c), they are attributable to minor species in equilibrium with the kinetic product **2**.

Attempts to obtain a pure sample of **2** were unsuccessful. The use of CH_3CN as a solvent led a mixture of 1-MeCy and *cis*-$[(PMe_2Ph)_2Pt(\mu\text{-OH})]_2(NO_3)_2$ (molar ratio 2:1) to dissolve in ca. 2 h at ambient conditions. The ^{31}P NMR spectrum of the resulting solution showed the presence of **1** in a yield of 95%. The remaining resonances were those of an AB multiplet at δ −18.09 and −19.5 ppm ($^2J_{PP}$ = 27.3 Hz), due to a yet unknown species, not observed after crystallization of the isolated crude product. Similarly, the ^{31}P NMR spectrum of the mixture obtained a few hours after mixing the reagents in D_2O indicated that complex **1** was the major component. In addition to the signals of **1** (Table 4), a very complex set of resonances in the range δ −18 to −24 ppm and an AB multiplet at δ −25.27 and −23.28 ppm ($^2J_{PP}$ = 25.6 Hz), tentatively attributed to the intermediate **2**, were detectable. In a few hours at ambient conditions, only the resonances of **1** were seen, as a result of the relatively fast conversion of **2**, and of others species in

Table 3. ^{1}H NMR Data (δ in ppm; J in Hz) for Complexes **1**−**3** in Various Solvents at 27 °C

compd	solvent	H6 ($^3J_{HH}$)	H5 ($^3J_{HH}$); [$^5J_{HP}$]	N4−H	NCH_3	PMe ($^2J_{HP}$)
1	DMSO-d_6	*a*	6.35 dd (7.1); [1.0]	6.63 br s	3.22 s	1.87 d (11.5); 1.43 d (11.4); 1.35 d (11.4); 1.16 d (10.8)
1	CD_3CN	7.13 d (7.5)	6.93 d (7.5); [1.5]	5.50 br s	2.56 s	1.81 d (11.6); 1.36 d (11.4); 1.36 d (11.4); 1.11 d (10.8)
1	$CDCl_3$	7.30 d (7.4)	6.45 dd (7.46); [1.6]	6.82 br s	3.42 s	1.836 d (8.8) and 1.408 d (12.6) (correlate with P_B); 1.449 d (12.1) and 1.18 d (10.5) (correlate with P_A)
2	DMSO-d_6	7.20 d (7.3)	ca. 5.90 d (7.2)	7.03 br s	3.12 s	2.003 d (10.5); 1.819 d (11.4); 1.518 d (10.5); 1.426 d (11.4)
3	$CDCl_3$	7.57[b]	6.87 dd (ca 7); [1.7]	6.84 br s	3.32	1.868 d (11.2); ca. 1.4 (correlate with P_B^I); 1.680 d (11.2); 1.314 d (10.8) (correlate with P_A^I)
		7.20 d (7.6)	6.79[b]	ca. 7.5	3.36	1.243 d (11.2); 0.977d (11.2) (correlate with P_A^{II}); 1.235 d (11.2); ca. 1.18 d (correlate with P_B^{II})
		7.6[b]	6.89 dd (7.4); [1.4]	6.66 br s	3.29	1.768 d (10.4);1.616 d (10.4); 1.599 d (10.8); 1.565 d (10.0) (correlate with P_A^{III} and P_B^{III})
3	DMSO-d_6	*a*	6.49 dd (6.49); [1.6]	6.60	3.16	1.885 d (11.4); 1.834 d (11.4); 1.640 d (11.2); 1.606 d (10.8); 1.549 d (11.4); 1.517 d (10.2)
		a	6.47 dd (8.0); [1.7]	6.33	3.13	1.389 d (10.8); 1.177 d (10.8); 1.126 d (11.4); 1.097 d (11.2); 1.050 d (11.4); 0.772 d (11.4)
		a	6.53 dd (7.80); [1.5]	*a*	ca. 3.4	

[a] Not attributed. [b] Values determined through COSY experiments.

Table 4. ^{31}P NMR Data (δ, in ppm; J in Hz; $^1J_{PPt}$ in Parentheses) for Complexes **1**−**3** in Various Solvents at 27 °C

complex (solvent)	$\delta(P_A)$	$\delta(P_B)$	$^2J_{PP}$
1 (DMSO-d_6)	−16.54 (3226)	−19.44 (3327)	24.8
1 (CD_3CN)	−17.48 (3222)	−20.46 (3336)	24.6
1 (D_2O)	−16.64 (3219)	−20.43 (3349)	24.7
1 ($CDCl_3$)	−17.83 (3221)	−21.11 (3334)	24.7
2 (DMSO-d_6)	−22.80 (3360)	−23.56 (3127)	25.5
3 ($CDCl_3$)	−16.70 (3230) I[a]	−20.70 (3291)	24.8
	−19.79 (3164) II	−20.05 (3164)	25.8
	−23.40 (3388) III	−25.70 (3370)	23.3
3 (DMSO-d_6)	−14.7 (3230) I[a]	−18.62 (3291)	25.3
	−18.51 (3171) II	−18.51 (3171)	25.8
	−22.70 (3413) III	−24.13 (3396)	23.3

[a] I−III refer to P_A and P_B in Chart 3.

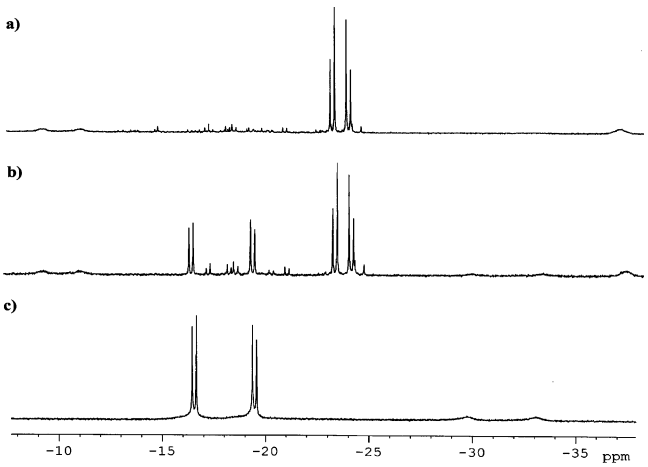

Figure 3. $^{31}P\{^1H\}$ NMR spectra (central part) of *cis*-$[(PMe_2Ph)_2Pt(\mu\text{-}OH)]_2(NO_3)_2$ and 1-MeCy (1:2 molar ratio) in DMSO-d_6 at 27 °C: (a) fresh solution; (b) after 45 h; (c) after 3 weeks at room temperature.

equilibrium, into the thermodynamically more stable trinuclear complex.

Although we were unable to obtain a suitable crystal of **2** for X-ray analysis, the comparison of the ^{31}P and ^{195}Pt NMR data with those of **1**, and with those found for the PMe_3 analogues,[11] strongly supports for **2** a dinuclear nature. As a matter of fact, the chemical shift difference of the ^{195}Pt NMR resonances in **1** (δ −4314 ppm) and **2** (δ −4139 ppm) is very similar to that found in the related PMe_3 analogues ($\Delta\delta$ 156 ppm).

Characterization of the Linkage Isomer of 1, 3. When the condensation reaction between *cis*-$[(PMe_2Ph)_2Pt(\mu\text{-}OH)]_2(NO_3)_2$ and 1-MeCy is carried out in chlorinated solvents, the main reaction product is the cyclic trinuclear complex **3**, the linkage isomer of **1** depicted in Chart 3. The structure of **3** has been elucidated through a detailed multinuclear NMR study, carried out in $CDCl_3$ and DMSO-d_6. The pertinent ^{1}H and ^{31}P NMR data are collected in Tables 3 and 4, respectively. At 600 MHz, the cytosinate ligands exhibit three sets of signals, in agreement with the presence of a different chemical environment for each nucleobase. Moreover, the methyl groups of each PMe_2Ph ligand show distinct resonances, giving a total of 12 doublets. As observed for complex **1**, the H5 resonances are characterized by doublets of doublets, while the N4−H protons show broad singlets in the range δ 6.6−7.5 ppm. Only one of the H6 resonances (doublet at δ 7.20 ppm, $^3J_{HH}$ = 7.6 Hz) was directly detectable in the 1D ^{1}H NMR spectrum. The remaining H6 resonances were obtained through COSY experiments. The attribution of the N4−H signals has been obtained on the basis of ^{15}N−^{1}H HMBC experiments (see the Supporting Information, Figure S3 and S4). Two N4−H protons (at δ 6.84 and 6.66 ppm, in $CDCl_3$) have chemical shifts very similar to that found for **1**, while the third (at ca. 7.5 ppm, overlapped by the phenyl resonances) appears to be particularly deshielded.

In the corresponding ^{31}P NMR spectrum, the phosphine ligands show three AB multiplets, labeled as A^IB^I, $A^{II}B^{II}$, and $A^{III}B^{III}$ (see Table 4), having the same relative intensities. 2D ^{31}P−^{1}H NMR heterocorrelated experiments indicate that *each* ^{31}P nucleus of the $A^{III}B^{III}$ multiplet correlates with a H5 proton, as shown in Figure 4 for the spectrum obtained in $CDCl_3$. In particular, the ^{31}P NMR resonances at δ −23.40 and −25.70 ppm correlate with the protons δ 6.79 and 6.87 ppm, respectively, indicating the presence of two nucleobases bonded at the same metal center, *both* coordinated at the N3 site. The remaining H5 proton shows correlation with the resonance at δ −20.70 ppm (P_B^I). The same results were obtained in DMSO-d_6. The two ligands labeled $P_A^{II}P_B^{II}$ (Chart 3), having chemical shifts only slightly different in chlorinated solvents (Table 4) or coincident (in DMSO-d_6, at 121

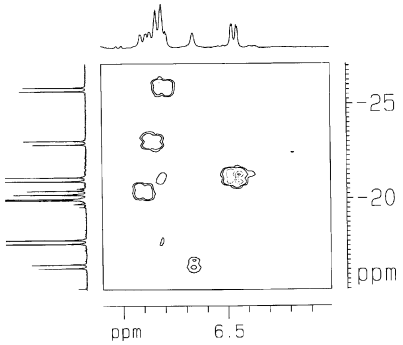

Figure 4. $^{31}P\{^1H\}-^1H$ HMBC spectra (low field) of **3** in $CDCl_3$.

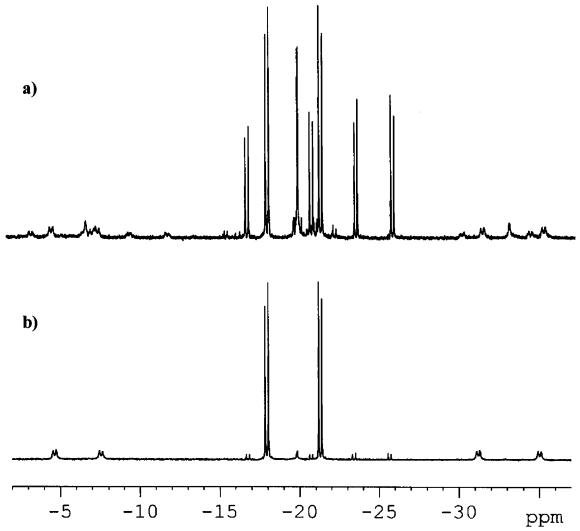

Figure 5. $^{31}P\{^1H\}$ NMR spectra of a solution of $[(PMe_2Ph)_2Pt(\mu\text{-}OH)]_2(NO_3)_2$ and 1-MeCy (1:2) in $CDCl_3$ at room temperature: (a) after 50 min; (b) after 24 h.

MHz), exhibit the lowest values of $^1J_{PPt}$ (3164 Hz in $CDCl_3$), as expected for phosphines in the trans position to N4-coordinated nucleobases.

In chlorinated solvents, complex **3** slowly isomerizes to **1**. Figure 5a shows the ^{31}P NMR spectrum of the mixture obtained 50 min after mixing the reagents in $CDCl_3$. The spectrum of the same solution, obtained after 24 h at ambient conditions (Figure 5b), shows that the isomerization of **3** is almost complete. Conversely, if the reaction is carried out on a larger scale (see the Experimental Section) in CH_2Cl_2, followed by the precipitation of the product with the addition of Et_2O, the ^{31}P NMR spectrum of the resulting solid, dissolved in $CDCl_3$, shows that the rate of conversion of **3** into **1** appears to be much decreased. The removal of water formed from the condensation reaction (eq 1) determines a sharp increase on the stability of **3**, whose initial concentration decreased only 15% after 8 days at room temperature. Because the isomerization of **3** requires dissociation of two Pt−N bonds (one Pt−N3 *and* one Pt−N4 bond), it is possible that in anhydrous solvents such a reaction is prevented. Moreover, a different pathway for the transformation of **3** into the stable isomer **1** is found in DMSO. In fact, when the isolated solid containing a mixture of **3** (65%) and **1** (35%) is dissolved in DMSO-d_6, we observe the progressive

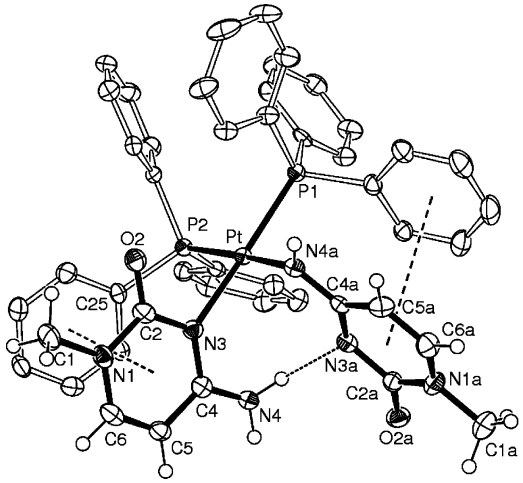

Figure 6. ORTEP drawing (ellipsoid at the 50% probability level) of the complex cation of **4** showing the intramolecular H bond and $\pi-\pi$ ring interactions.

Table 5. Selected Coordination Bond Distances (Å) and Angles (deg) for **4**

Pt−N3	2.100(3)	Pt−P1	2.2717(10)
Pt−N4a	2.061(4)	Pt−P2	2.2730(14)
N3−Pt−N4a	87.51(13)	N4a−Pt−P1	84.95(9)
N3−Pt−P1	169.97(10)	N4a−Pt−P2	176.48(9)
N3−Pt−P2	89.16(10)	P1−Pt−P2	98.22(4)

appearance of the dinuclear species **2** (not observed in chlorinated solvents), *followed* by its slow conversion into **1**.

Characterization of the Bis-adduct 4. Unlike the PMe_3 and PMe_2Ph analogues, the hydroxo complex containing PPh_3 reacts with 1-MeCy, in DMSO and chlorinated solvents, according to eq 2. The elemental analysis and X-ray structure

$$cis\text{-}[(PPh_3)_2Pt(\mu\text{-}OH)]_2^{2+} + 4(1\text{-MeCy}) \rightarrow 2(cis\text{-}[(PPh_3)_2Pt\{1\text{-MeCy}(-H)\}(1\text{-MeCy})]^+) + 2H_2O \quad (2)$$

determination of the isolated solid, after crystallization from DMF, is consistent with the formula *cis*-$[(PPh_3)_2Pt\{1\text{-MeCy}(-H)\}(1\text{-MeCy})]NO_3\cdot H_2O\cdot DMF$ (**4**·H_2O·DMF). The RX diffraction analysis, performed on a crystal of small dimensions, evidences that compound **4** is comprised of cationic complexes, NO_3^- anions, lattice water, and DMF molecules. The Pt metal exhibits the expected square-planar geometry, with a cytosine base coordinated through the endocyclic nitrogen N3 and the other through the deprotonated exocyclic amino group N4a, as shown in Figure 6 and Table 5. To the best of our knowledge, this is the first example of a structurally characterized Pt complex with N3 and N4 coordinated nucleobases in the cis position.[22] The Pt−N3 bond length of 2.100(3) Å appears to be significantly longer than the Pt−N4a one [2.061(4) Å], confirming the trend also found in the trinuclear complex **1** and in the neutral complexes *trans*-$[PtX_2(1\text{-MeCy},N^3)(1\text{-MeCy},N^4)]$ (X = Cl, I) recently described. The N3 and N4a coordinated bases form dihedral angles of 87.66(7) and 76.35(7)°, respectively,

(22) Miguel, P. J. S.; Lax, P.; Willermann, M.; Lippert, B. *Inorg. Chim. Acta* **2004**, *357*, 4552.

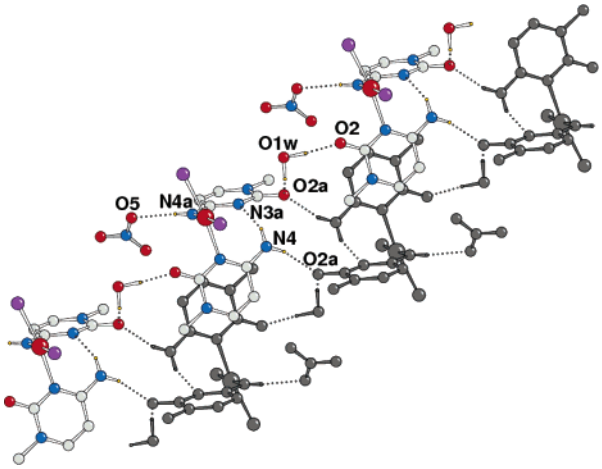

Figure 7. Crystal packing with an indication of H bonds (dotted lines) occurring along and between two arrays of complexes **4** (phosphine phenyl rings are not depicted for clarity).

with the mean coordination plane N_2P_2, with the larger tilting of the second (from the ideal perpendicular position) likely being assumed in order to favor the intramolecular H bond (see below).

As is evident from Figure 6, both of the bases are involved in $\pi-\pi$ interaction with an adjacent PPh_3 phenyl ring, with the distances between the ring centroids being 3.347(3) and 3.653(3) Å for the N3 and N4a coordinated bases, respectively. Moreover, the complex appears to be stabilized by an intramolecular H bond occurring between the N4 amino group and the uncoordinated nitrogen N3a [N···N distance 2.843(6) Å, N−H···N 147(4)°].

The crystal packing (Figure 7) shows complexes running along the *a* axis and bound by the lattice water molecules that join carbonyl groups of two consecutive complexes. The complexes of adjacent arrays are connected through H bonds occurring via N4−H···O2a and through $\pi-\pi$ interactions involving symmetry-related N3 coordinated bases, with the distance between the ring centroids being 3.619(3) Å. Finally, N4a acts as a H donor toward the nitrate oxygen O5. The DMF molecules are far apart and do not interact with the metal complexes.

Compound **4**, virtually insoluble in chlorinated solvents, has been characterized in DMSO-d_6 and DMF-d_7. The ^{1}H NMR spectrum shows two sets of resonances for the nucleobases: the H5 proton of the N3 platinated molecule (attributed through the COSY experiment; see the Supporting Information, Figure S5) exhibits a long-range ^{1}H−^{31}P coupling ($^5J_{HP}$ = 1.6 Hz) (not observed when the nucleobase is N4-coordinated), while the exocyclic amino protons appear as broad singlets at δ 8.34 and 10.63 ppm. Their attribution stems on the ^{15}N−^{1}H HMBC spectrum, shown in Figure 8, where these signals show a correlation with the same ^{15}N nucleus (at δ −261 ppm, $^1J_{NH}$ = ca. 80 Hz). The imino proton of 1-MeCy(−H), at δ 5.07 ppm, exhibits coupling with one of the ^{31}P nuclei ($^3J_{HP}$ = 4.7 Hz) and correlates with the ^{15}N NMR resonance at δ −275 ppm ($^1J_{NH}$ and $^2J_{NP}$ = ca. 85 and 90 Hz, respectively). In the ^{31}P NMR spectrum, the two phosphines exhibit two well-separated doublets at δ 12.34 and 0.21 ppm, the first of which shows a correlation

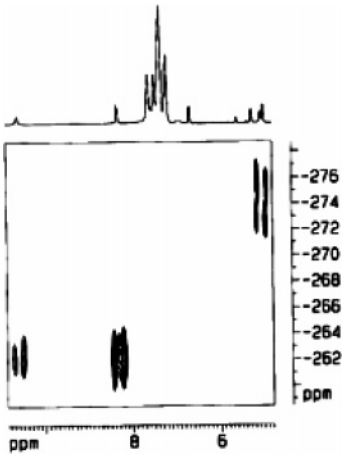

Figure 8. ^{15}N−^{1}H HMBC spectra (low field) of **4** in DMSO-d_6.

with the N4−H proton at δ 5.07 ppm, indicating a trans configuration of this phosphine with the N4-platinated nucleobase. As is observed in **1**, this ligand is at a lower field and experiences the lower $^1J_{PPt}$ value.

One of the exocyclic NH_2 protons appears particularly deshielded (δ 10.94 ppm, in DMF-d_7) when compared with the values found for N3-bonded 1-MeCy ligands in the bis-adducts *cis*-$[L_2Pt(1\text{-MeCy})_2]^{2+}$ (L = PMe_2Ph, δ 7.85 and 8.84 ppm)[15] and related complexes.[22] This result is in line with the presence of a strong intramolecular H bond as observed in the solid state.

No stable polynuclear complexes can be obtained with a lower nucleobase/Pt ratio. Complex **4**, in fact, is the main component of the reaction mixture even if the molar ratio is that of eq 1. This is likely due to the higher steric hindrance of the PPh_3 ligands, which prevent the 1-MeCy(−H) anion from behaving as bridging (or chelating ligand), leaving the fourth position around the metal ion available for coordination of a neutral molecule of the nucleobase.

Conclusions

The results here described lead to the conclusion that the deprotonation of the model nucleobase 1-MeCy promoted by the hydroxo ligands in *cis*-$[L_2Pt(\mu\text{-OH})]_2(NO_3)_2$ generates cytosinate ions that behave as mono- or bidentate ligands toward the metal center, depending on the ancillary ligands L. The more basic phosphines (PMe_3 and PMe_2Ph) form adducts in which the nucleobase acts as a bidentate ligand, bridiging the metals through the N3 and N4 atoms. The resulting products are the relatively stable (L = PMe_3) or scarcely stable (L = PMe_2Ph) *head-to-tail* dinuclear intermediates *cis*-$[L_2Pt\{1\text{-MeCy}(-H),N^3N^4\}]_2^{2+}$ that undergo rearrangement to the stable trinuclear cyclic analogues *cis*-$[L_2Pt\{1\text{-MeCy}(-H),N^3N^4\}]_3^{3+}$.

A linkage isomer of these trinuclear cycles has been characterized when the condensation reaction between the hydroxo complex stabilized by PMe_2Ph and the nucleobase is carried out in chlorinated solvents. In this case, the fast self-assembly of the $\{cis\text{-}L_2Pt^{2+}\}$ units with the cytosinate ions leads exclusively to *trinuclear* cyclic adducts, with the kinetically favored formation of the *unsymmetrical* isomer **3**. The subsequent quantitative conversion of **3** into the

thermodynamically stable isomer **1** is a clear indication of the more favorable arrangement of the ligands when the nucleobases bridge the metals *symmetrically*.

In contrast, the presence of the sterically demanding PPh_3 ligands in *cis*-$[L_2Pt(\mu\text{-}OH)]_2(NO_3)_2$ favors a monodentate behavior of the cytosinate ion, which binds the metal at the N4 site. The concomitant coordination of a second molecule of cytosine stabilizes the mononuclear adduct *cis*-$[(PPh_3)_2Pt\{1\text{-}MeCy(-H)\}(1\text{-}MeCy)]^+$ through a strong intramolecular H bond.

Acknowledgment. This work was financially supported by the Ministero dell'Università e della Ricerca Scientifica e Tecnologica (PRIN 2004). We are indebted to Dr. E. Marotta for mass spectra.

Supporting Information Available: X-ray crystallographic data in CIF format, ESI and COSY spectra, and kinetic study of the conversion of **2** into **1**. This material is available free of charge via the Internet at http://pubs.acs.org.

IC060831R